Journal of Alloys and Compounds 489 (2010) 293–296

Contents lists available at ScienceDirect

Journal of Alloys and Compounds

journal homepage: www.elsevier.com/locate/jallcom

Growth and spectroscopic characteristics of Cr^{3+}:$CsAl(MoO_4)_2$ crystal

Guojian Wang, Lizhen Zhang, Zhoubin Lin, Guofu Wang*

State Key Laboratory of Structural Chemistry, Fujian Institute of Research on the Structure of Matter, Chinese Academy of Sciences, No 155 Yangqiao Xilu, Fuzhou, Fujian 350002, China

ARTICLE INFO

Article history:
Received 12 June 2009
Received in revised form
15 September 2009
Accepted 16 September 2009
Available online 23 September 2009

PACS:
42.70.Hj
65.40.De
78.20.−e

Keywords:
Crystal growth
Photoelectron spectroscopic

ABSTRACT

This paper reports the growth and spectroscopic characteristics of Cr^{3+}:$CsAl(MoO_4)_2$ crystal. A Cr^{3+}:$CsAl(MoO_4)_2$ crystal with dimensions of 42 mm × 37 mm × 10 mm has been successfully grown from a flux of $Cs_2Mo_3O_{10}$ by the TSSG method. The absorption and emission spectra were investigated. The absorption cross sections σ_a are 5.05×10^{-20} cm^{-2} at 481 nm for the $^4A_2 \rightarrow {}^4T_1$ transition and 3.06×10^{-20} cm^{-2} at 670 nm for the $^4A_2 \rightarrow {}^4T_2$ transition of Cr^{3+} ions, respectively. The emission cross section σ_e of $^4T_2 \rightarrow {}^4A_2$ transition is 4.27×10^{-20} cm^2 at 818 nm and fluorescence lifetime is 21 μs. Based on the absorption and emission spectra, the crystal field strength Dq, the Racah parameters *B* and *C*, the effective phonon energy $\hbar\omega$ and the Huang–Rhys factor *S* were calculated. The investigated results show that Cr^{3+}:$CsAl(MoO_4)_2$ crystal may be regarded as a potential tunable laser crystal material.

1. Introduction

Since tunable solid-state lasers have a wide field application in medicine, ultra short pulse generation, environment and communication, research on Cr^{3+}-doped tunable solid-state laser in the visible and near infrared spectrum has gained strong interest [1–5]. Recently double metals molybdate and tungstate with a general formula $M^IM^{III}(M^{VI}O_4)_2$ (where M^I = Na, K, Rb, Cs, M^{III} = Al, In, Sc and M^{VI} = Mo, W)are gaining attentions because their interesting chemical and physical properties. The Cr^{3+}-doped $M^IM^{III}(M^{VI}O_4)_2$ materials have currently receiving a great deal of attention due to their interesting properties in tunable laser applications [6–16]. $CsAl(MoO_4)_2$ is a member of this family of materials with $P\bar{3}m1$ space group and cell parameters $a = 5.551(1)$ Å, $c = 8.037(2)$ Å [17]. It was reported that single crystals of Cr^{3+}-doped $CsAl(MoO_4)_2$ were grown using the Klevtsov method [18] by Hermanowicz [6]. However, the crystals with large size and high quality were difficulty obtained by this method. In this paper, we report the growth of Cr^{3+}:$CsAl(MoO_4)_2$ crystal by TSSG technique and its spectroscopic characterization.

2. Crystal growth

Since $CsAl(MoO_4)_2$ crystal melts incongruently at 715 °C [19], Cr^{3+}-doped $CsAl(MoO_4)_2$ crystals were only grown by the top seed solution growth (TSSG) method. Cr^{3+}-doped $CsAl(MoO_4)_2$ crystals were grown from a flux of $Cs_2Mo_3O_{10}$ by the TSSG method. In order to select the suitable composition of solution, the solubility curve of $CsAl(MoO_4)_2$ in $CsAl(MoO_4)_2$–$Cs_2Mo_3O_{10}$ solution was determined by means of trial seeding. The saturation temperatures were determined for various compositions in a range of 60–80 mol% $Cs_2Mo_3O_{10}$ by adjusting the temperature of the solution until a trial seeding showed no change in weight or surface micro-topography after 4–5 h immersion. Fig. 1 shows the solubility curve of $CsAl(MoO_4)_2$ in the solution.

The crystal growth was carried out in a vertical tubular muffle furnace with a nikel-chrome wire as the heating element. An AL-708 controller controlled the furnace temperature and the rate of cooling. The crystal was grown in a platinum crucible with dimensions of ⌀ 60 mm × 50 mm. The starting materials with 66.7 mol% $Cs_2Mo_3O_{10}$ and 33.3 mol% $CsAl(MoO_4)_2$ were weighed according to following chemical reaction equations:

$$Cs_2CO_3 + (1-x)Al_2O_3 + xCr_2O_3 + 4MoO_3 = 2CsAl_{1-x}Cr_x(MoO_4)_2 + CO_2 \quad (1)$$

$$Cs_2CO_3 + 3MoO_3 = Cs_2Mo_3O_{10} + CO_2 \quad (2)$$

* Corresponding author. Tel.: +86 591 83714636; fax: +86 591 83714636.
E-mail address: wgf@ms.fjirsm.ac.cn (G. Wang).

0925-8388/$ – see front matter © 2009 Elsevier B.V. All rights reserved.
doi:10.1016/j.jallcom.2009.09.076

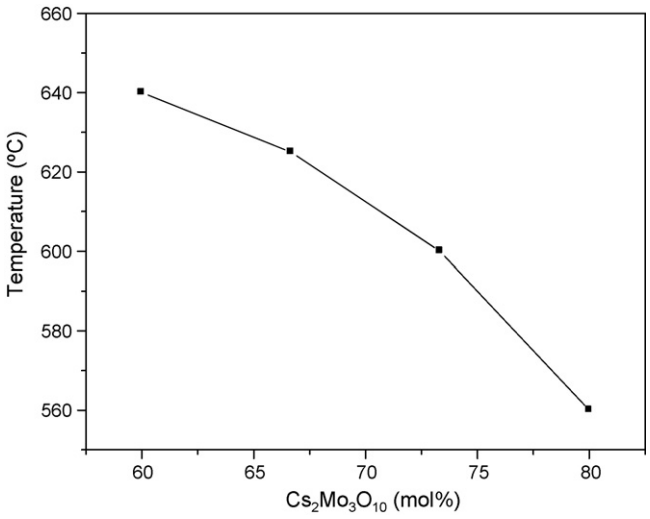

Fig. 1. Solubility curve of $CsAl(MoO_4)_2$ in $CsAl(MoO_4)_2$–$Cs_2Mo_3O_{10}$ solution.

The chemicals used were Cs_2CO_3, Al_2O_3 and MoO_3 with 99.95% purity and Cr_2O_3 with 99.99% purity. The weighed materials with 1 at.% Cr_2O_3 were mixed and put into the platinum crucible. The mixture of starting materials was kept at temperature 30 °C above the saturation temperature for 2 days to make the solution melt completely and homogeneously. The saturation temperature of the solution was exactly determined by repeated seeding. The crystal was grown at a cooling rate of 1–2 °C/day and rotated at a rate of 4.5 rpm. When the growth process was ended, the crystal was drawn out of the solution surface and cooled down to room temperature. Cr^{3+}:$CsAl(MoO_4)_2$ crystal with dimensions of 42 mm × 37 mm × 10 mm was obtained, as shown in Fig. 2. During the cooling process Cr^{3+}:$CsAl(MoO_4)_2$ crystals strongly tended towards cracking and cleaving. In $CsAl(MoO_4)_2$ crystals, MoO_4 tetrahedra and AlO_6 octahedra built up a $[AlMo_2O_8{}^{-1}]$ layer, the $[AlMo_2O_8{}^{-1}]$ layers are perpendicular to the trigonal *c*-axis [17,20]. Since this layer structure of $CsAl(MoO_4)_2$ crystals easily results in cleave along the $[AlMo_2O_8{}^{-1}]$ layer, the grown $CsAl(MoO_4)_2$ crystals tended towards cleaving during the cooling process under thermal stress. The cleavage plane of Cr^{3+}:$CsAl(MoO_4)_2$ crystal was determined to belong to (0 0 1) face using an YX-200 X-ray diffraction orientating instrument. The appeared faces of the grown crystal of Cr^{3+}:$CsAl(MoO_4)_2$ crystal were determined by the

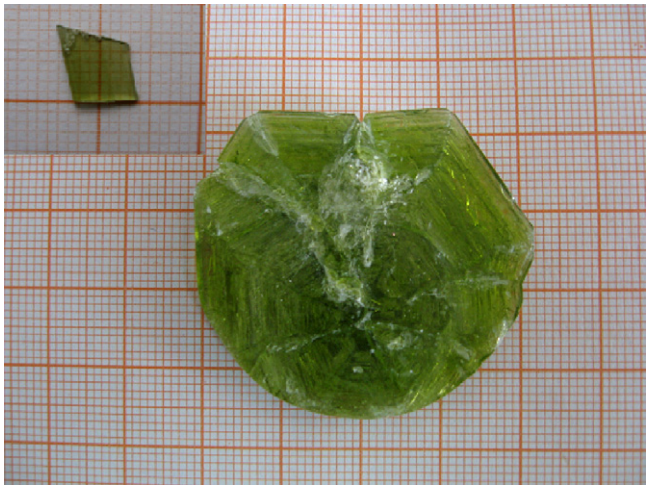

Fig. 2. Photograph of the grown Cr^{3+}:$CsAl(MoO_4)_2$ crystal.

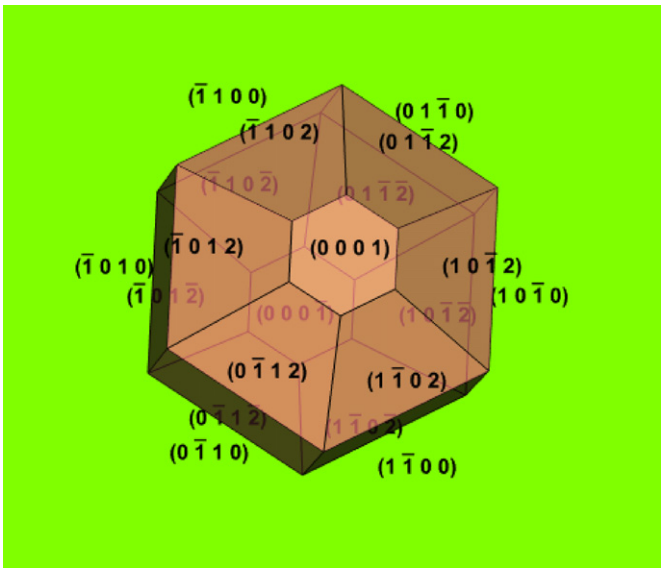

Fig. 3. Growth morphology of Cr^{3+}:$CsAl(MoO_4)_2$ crystals.

YX-200 X-ray diffraction orientating instrument, which belong to (0 0 1), (1 0 2) and (1̄ 1 0), respectively. Based on the structure of $CsAl(MoO_4)_2$, the morphological scheme of $CsAl(MoO_4)_2$ crystal is drawn by WinXMorph program [21], as shown in Fig. 3.

The Cr^{3+} ions concentration in Cr^{3+}:$CsAl(MoO_4)_2$ crystal was determined to be 2.0 at.% by ionic coupled plasma (ICP) spectrometry. The distribution coefficient is defined as following formula:

$$\eta = \frac{Cr^{3+}\ \text{concentration in the crystal}}{Cr^{3+}\ \text{concentration in the initial charge}} \quad (3)$$

Thus, the distribution coefficient of Cr^{3+} ion in Cr^{3+}:$CsAl(MoO_4)_2$ crystals is 2.0.

The specific heat was measured using a NETZSCH STA 449C simultaneous thermal analyzer. Fig. 4 shows the dependence of the specific heats of Cr^{3+}:$CsAl(MoO_4)_2$ crystals on the temperature. The specific heat is 0.27 J/g K at 50 °C.

3. Spectral properties

A sample with dimensions of 5.0 mm × 5.2 mm × 1 mm was cut from the as-grown crystal and polished for the spectral measurement. The absorption spectrum at room temperature was recorded with a PerkinElmer UV–VIS–NIR Spectrometer (Lambda-900). The

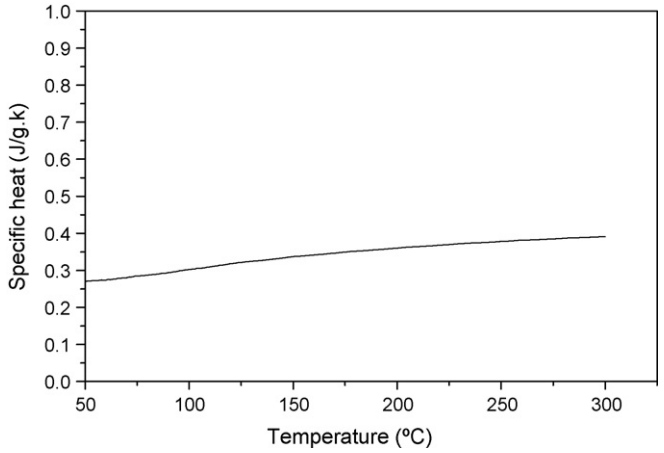

Fig. 4. Dependence of the specific heat on the temperature.

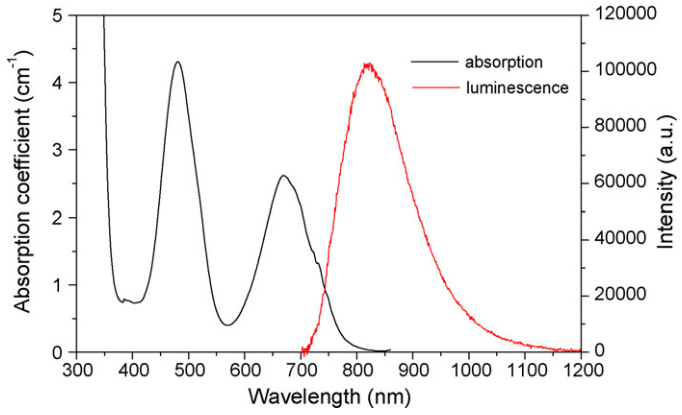

Fig. 5. Absorption and luminescence spectra of Cr^{3+}:$CsAl(MoO_4)_2$ crystal at room temperature.

fluorescence spectrum and fluorescence lifetime were measured using an Edinburgh Instruments FLS920 spectrophotometer with a continuous Xe-flash lamp at room temperature.

Fig. 5 shows the absorption and luminescence spectra of Cr^{3+}:$CsAl(MoO_4)_2$ crystal. The Cr^{3+} as an active ion tends to be incorporated into environments which are octahedrally coordinated by ligands. Since in the structure of $CsAl(MoO_4)_2$ there is only one kind of AlO_6 octahedron, the absorption spectrum of Cr^{3+}:$CsAl(MoO_4)_2$ should be originated from one center of Cr^{3+} ions. The absorption spectrum consists of two broad bands, corresponding to the $^4A_2 \rightarrow {}^4T_1$ transition of Cr^{3+} ion and to the $^4A_2 \rightarrow {}^4T_2$ transition of Cr^{3+} ion, respectively. The absorption cross section σ_a were determined using $\sigma_a = \alpha/N_c$, where α is the absorption coefficient, N_c is the concentration of Cr^{3+} ions in Cr^{3+}:$CsAl(MoO_4)_2$, which is 8.56×10^{19} ions/cm^3. Then the absorption cross section σ_a is 5.05×10^{-20} cm^{-2} at 481 nm for the $^4A_2 \rightarrow {}^4T_1$ transition and 3.06×10^{-20} cm^{-2} at 670 nm for the $^4A_2 \rightarrow {}^4T_2$ transition, respectively. The peak at 738.12 nm is attributed to $^4A_2 \rightarrow {}^2E$ transition of Cr^{3+} ion [6].

The energies of the electronic states of Cr^{3+} ion, which are determined by the crystal field Dq and Racah parameters B and C. According to the Tanabe and Sugano diagram [22], a strong crystal field is present when $Dq/B > 2.3$. In this case the $^4T_2$ level is above ^2E level, the R-line and its vibronic sideband is only observed. For example, the laser action of ruby (Cr^{3+}:Al_2O_3) is driven by the $^2E \rightarrow {}^4A_2$ R-line emission. When $Dq/B < 2.3$, the crystal field is weak. The $^4T_2$ level is below ^2E level, the broad emission band of $^4T_2 \rightarrow {}^4A_2$ transition is only observed as observed for Cr:LiCAF and Cr:LiSAF crystals. Then the $^4T_2$ level is the lower one and a broadband luminescence is observed. There are also intermediate field materials where $Dq/B \sim 2.3$.

The strength of the crystal field Dq and Racah parameters B and C can be obtained from the absorption. The energy separations of the $^4T_1$ and $^4T_2$ states from $^4A_2$ ground state are very sensitive to Dq, the strength of the crystal field. The peak energy of $^4A_2 \rightarrow {}^4T_2$ transition measures 10Dq, i.e. $10Dq = E_a(^4T_2)$. The energy at the peak of the $^4A_2 \rightarrow {}^4T_2$ band depends on the both Dq and B [22,23]. If ΔE is the difference in energy at peaks of the two bands, i.e. $\Delta E = E_a(^4T_1) - E_a(^4T_2)$, then substituting the measured values of $\Delta E = 5865$ cm^{-1} and $Dq = 1492.5$ cm^{-1} into Eq. (4), determines B to be 583.1 cm^{-1}.

$$\frac{B}{Dq} = \frac{(\Delta E/Dq)^2 - 10(\Delta E/Dq)}{15((\Delta E/Dq) - 8)} \quad (4)$$

The C can be calculated from following formula [14]:

$$C = \frac{E(^2E) - 7.9B + 1.8B^2/Dq}{3.05} \quad (5)$$

Table 1
Energy levels of Cr^{3+} ion in Cr^{3+}:$CsAl(MoO_4)_2$ crystal.

O_h group show $^{2S+1}\Gamma_i$	Level	Energy (cm^{-1})	Energy of relative ground state (cm^{-1})
$^2T_2(a^2D,b^2D,^2F,^2G,^2H)$	t_2^3	−6,437	20,219
	$t_2^2(^3T_1)e$	1,661	28,317
	$t_2^2(^1T_2)e$	10,243	36,899
	$t_2e^2(^1A_1)$	35,874	62,530
	$t_2e^2(^1E)$	18,079	44,735
$^2T_1(^2P,^2F,^2G,^2H)$	t_2^3	−12,630	14,026
	$t_2^2(^3T_1)e$	6,099	31,960
	$t_2^2(^1T_2)e$	1,992	28,648
	$t_2e^2(^3A_2)$	16,573	43,229
	$t_2e^2(^1E)$	22,294	48,950
$^2E(a^2D,b^2D,^2G,^2H)$	t_2^3	−13,122	13,534
	$t_2^2(^3A_1)e$	19,306	45,962
	$t_2^2(^3E_1)e$	3,583	29,378
	e^3	38,192	64,848
$^4T_1(^4P,^4F)$	$t_2^2(^3T_1)e$	−5,867	20,789
	$t_2e^2(^3A_2)$	6,075	32,731
$^4T_2(^4F)$	$t_2^2(^3T_1)e$	−11,731	14,925
$^2A_1(^2G)$	$t_2^2(^1E_1)e$	−201	26,455
$^2A_2(^2F)$	$t_2^2(^1E_1)e$	11,461	38,117
$^4A_2(^4F)$	t_2^3	−26,656	0

Using the value $E(^2E) = 13{,}548$ cm^{-1} and the values of Dq and B, the C was calculated to be 3066 cm^{-1}.

The energy levels of Cr^{3+}:$CsAl(MoO_4)_2$ crystal can be calculated when the values of Dq, B and C are substituted in the secular equation [24]. Then the energy levels of Cr^{3+}:$CsAl(MoO_4)_2$ crystal are listed in Tables 1 and 2 show the calculated values are in good agreement with the experimental values for Cr^{3+}:$CsAl(MoO_4)_2$ crystal.

The luminescence spectrum of Cr^{3+}:$CsAl(MoO_4)_2$ crystal excited with 670 nm radiation at room temperature is shown in Fig. 5. The dominant feature of luminescence of Cr^{3+}:$CsAl(MoO_4)_2$ crystal is broad emission band with peak at 818 nm, corresponding to the $^4T_2 \rightarrow {}^4A_2$ transition. $Dq/B = 2.55 > 2.3$ of Cr^{3+}:$CsAl(MoO_4)_2$ crystal implies that the energy level of $^4T_2$ is higher than that of ^2E, therefore, the line emission of $^2E \rightarrow {}^4A_2$ transition should be visible. However, only the $^4T_2 \rightarrow {}^4A_2$ transition is observed on the photoluminescence spectrum at 300 K. This could be explained by the increased thermal population of the $^4T_2$ level with increasing temperature as well as by two orders of magnitude greater probability for the $^4T_2 \rightarrow {}^4A_2$ transition than that for the $^2E \rightarrow {}^4A_2$ transition to take place [11]. These means Cr^{3+} ions occupy intermediate crystal field sites in Cr^{3+}:$CsAl(MoO_4)_2$ crystal.

The emission cross section σ_e was determined by the following formula [25]:

$$\sigma_e = \frac{\lambda^2}{4\pi^2 \tau_f n^2 \Delta\upsilon} \quad (6)$$

where n is refractive index which was estimated to be 1.72 by Abbe Refractometer at 589 nm wavelength. λ is the emission wavelength, the $\Delta\nu$ is the half-band frequency and τ_f is fluorescence lifetime. The luminescence lifetime of $^4T_2 \rightarrow {}^4A_2$ transition was measured to be 21 μs, as shown in Fig. 6. Then, the emission cross section σ_e at 818 nm is 4.27×10^{-20} cm^2.

Table 2
Theory and experiment values of Cr^{3+}:$CsAl(MoO_4)_2$ crystal.

Level	Theory value (cm^{-1})	Experiment values (cm^{-1})	Relative error (%)
$^2E(t_2^3)$	13,534	13,548	0.1
$^4T_2(t_2^2(^3T_1)e)$	14,925	14,925	0
$^4T_1(t_2^2(^3T_1)e)$	20,789	20,790	0.005

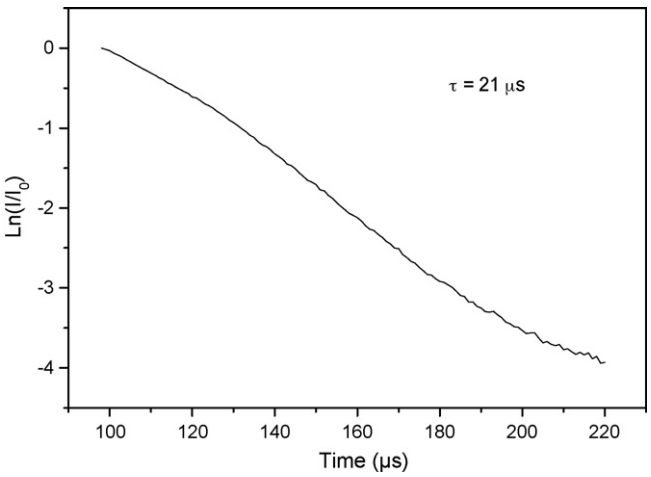

Fig. 6. Luminescence decay curve of Cr^{3+}:$CsAl(MoO_4)_2$ crystal at room temperature.

Having luminescence spectrum, the effective phonon energy $\hbar\omega$ and the Huang–Rhys factor S can be obtained. For oxides the effective phonon energy can be expressed in the following equation [26]:

$$\hbar\omega \approx 2.25\,E_a\left[\frac{0.3456}{E_a - E_e}\right]^{1/2} \quad (7)$$

where E_a is the peak energy absorption spectrum ($^4A_2 \rightarrow {}^4T_2$ transition) and E_e is the peak energy of emission spectrum($^4T_2 \rightarrow {}^4A_2$ transition).

The Huang–Rhys factor S is related with the difference in energy between the absorption and emission band peaks (Stokes shift, $E_s = E_a - E_e$) by following expression [26]:

$$E_s = 2S\hbar\omega \quad (8)$$

Thereupon, $E_s = 2700\,cm^{-1}$, $\hbar\omega = 379.9\,cm^{-1}$ and $S = 3.55$ can be obtained by the experimental values of $E_a = 14{,}925\,cm^{-1}$ and $E_e = 12{,}225\,cm^{-1}$. Cr^{3+} ions in $CsAl(MoO_4)_2$ crystal have a stronger coupling to the crystal lattice than that in other some fluoride crystals (such as K_2NaScF_6, ScF_3, K_2NaGaF_6, etc.) [26].

4. Conclusion

A Cr^{3+}:$CsAl(MoO_4)_2$ crystal with dimensions of 42 mm × 37 mm × 10 mm has been grown from a flux of $Cs_2Mo_3O_{10}$ by the TSSG method. The solubility curve of $CsAl(MoO_4)_2$ in the $CsAl(MoO_4)_2$–$Cs_2Mo_3O_{10}$ solution was measured. The distribution coefficient of Cr^{3+} ion in Cr^{3+}:$CsAl(MoO_4)_2$ crystals is 2.0 which is over 1.0. Such large coefficient shows that the Cr^{3+} ions $CsAl(MoO_4)_2$ crystal are easily incorporated into $CsAl(MoO_4)_2$ crystal, but it may result in the inhomogeneous distribution of Cr^{3+} ions in Cr^{3+}:$CsAl(MoO_4)_2$ crystal. Based on the absorption and emission spectra, the crystal field strength Dq, the Racah parameters B and C, the effective phonon energy $\hbar\omega$ and the Huang–Rhys parameter S were calculated: Dq = 1492.5 cm^{-1}, B = 583.1 cm^{-1} and C = 3066 cm^{-1}, $\hbar\omega$ = 379.9 cm^{-1} and the Huang–Rhys parameter S = 3.55. The absorption cross section σ_a of $^4A_2 \rightarrow {}^4T_1$ and $^4A_2 \rightarrow {}^4T_2$ transitions are 5.05×10^{-20} cm^{-2} and 3.06×10^{-20} cm^{-2}, respectively. The large absorption cross sections mean that is suitable for efficient pumping with commercial laser diodes such as AlGaInP whose emission wavelength ranges 670–690 nm. At room temperature the luminescence spectrum of Cr^{3+}:$CsAl(MoO_4)_2$ crystal has a broad emission of wide tunable range (700–1200 nm) with FWHM of 147 nm. The emission cross section σ_e of $^4T_2 \rightarrow {}^4A_2$ transition is 4.27×10^{-20} cm^2 and fluorescence lifetime is 21 μs. In conclusion, the investigated results show that Cr^{3+}:$CsAl(MoO_4)_2$ crystal may be regarded as a potential tunable laser crystal material.

Acknowledgments

This work is supported by the National Natural Science Foundation of China (No. 60978054) and the Young Scientists Innovation Foundation of Fujian Province (2008F3113), respectively.

References

[1] G.J. Wang, Z.B. Lin, L.Z. Zhang, Y.S. Huang, G.F. Wang, J. Lumin. 129 (2009) 1398.
[2] E. Cavalli, A. Belletti, M.G. Brik, J. Phys. Chem. Solids 69 (2008) 29.
[3] D. Ivanova, V. Nikolov, R. Todorov, J. Cryst. Growth 311 (2009) 3428.
[4] U. Demirbas, A. Sennaroglu, F.X. Kärtner, J.G. Fujimoto, J. Opt. Soc. Am. B 26 (2009) 64.
[5] U. Demirbas, A. Sennaroglu, F.X. Kärtner, J.G. Fujimoto, Opt. Lett. 34 (2009) 497.
[6] K. Hermanowicz, J. Lumin. 109 (2001) 9.
[7] K. Hermanowicz, M. Maczka, M. Deren, J. Hanuza, W. Strek, H. Drulis, J. Lumin. 92 (2001) 151.
[8] K. Hermanowicz, J. Alloys Compd. 341 (2001) 179.
[9] W.C. Zhang, Q. Zhou, M. Yang, X.X. Wu, Opt. Mater. 27 (2004) 449.
[10] A. Peña, R. Solé, J. Gavaldà, F. Massons, F. Díaz, M. Aguiló, Chem. Mater. 18 (2006) 442.
[11] I. Nikolov, X. Mateos, F. Güell, J. Massons, V. Nikolov, P. Peshev, F. Díaz, Opt. Mater. 25 (2004) 53.
[12] K. Hermanowicz, J. Hanuza, M. Maczka, P.J. Dereń, E. Mugeński, H. Drulis, I. Sokolska, J. Sokolnicki, J. Phys Condens. Matter 13 (2001) 5807.
[13] A.J. Mao, X.Y. Kuang, H. Wang, X.F. Huang, J. Alloys Compd. 448 (2008) 6.
[14] G.J. Wang, X.F. Long, L.Z. Zhang, G.F. Wang, J. Cryst. Growth 310 (2008) 624.
[15] G.J. Wang, X.F. Long, L.Z. Zhang, G.F. Wang, S. Polosan, T. Tsuboi, J. Lumin. (2008) 1556.
[16] G.J. Wang, X.M. Han, M.J. Song, Z.B. Lin, G.F. Wang, X.F. Long, Mater. Lett. 61 (2007) 3886.
[17] P.E. Tomaszewski, A. Pieteraszko, M. Maczka, J. Hanuza, Acta Crystallogr. E58 (2002) I119.
[18] P.V. Klevtzov, L.P. Kozeeva, L.Y. Khartchenko, Kristallografiya 20 (1975) 1210.
[19] V.K. Trunov, V.A. Efremov, Zh. Neorgan, Khim. 16 (1971) 2026.
[20] P.V. Klevtsov, R.F. Klevtsova, J. Struct. Chem. 18 (1977) 339.
[21] W. Kaminsky, J. Appl. Cryst. 40 (2007) 382.
[22] Y. Tanabe, S. Sugano, J. Phys. Soc. Jpn. 9 (1954) 753.
[23] B. Henderson, G.F. Imbush, Optical Spectroscopy of Inorganic Crystals, Oxford University Press, Oxford, 1989.
[24] Y. Tanabe, S. Sugano, J. Phys. Soc. Jpn. 9 (1954) 766.
[25] X.F. Long, Z.B. Lin, Z.S. Hu, G.F. Wang, Chem. Phys. Lett. 392 (2004) 192.
[26] Z.D. Luo, Y.D. Huang, J. Phys. Condens. Matter 5 (1993) 9411.